Cancer Immunology, Immunotherapy (2024) 73:82
https://doi.org/10.1007/s00262-024-03673-x

RESEARCH

DR30318, a novel tri-specific T cell engager for Claudin 18.2 positive cancers immunotherapy

Zhe Ma[1,2] · Zhenxing Zhou[2] · Wenwen Duan[2] · Gaofeng Yao[2] · Shimei Sheng[2] · Sidou Zong[2] · Xin Zhang[2] · Changkui Li[2] · Yuanyuan Liu[2] · Fengting Ou[5] · Maha Raja Dahar[1] · Yanshan Huang[2] · Lushan Yu[1,3,4,5,6]

Received: 20 February 2024 / Accepted: 8 March 2024 / Published online: 30 March 2024

Abstract

Background Claudin 18.2 (CLDN18.2) is a highly anticipated target for solid tumor therapy, especially in advanced gastric carcinoma and pancreatic carcinoma. The T cell engager targeting CLDN18.2 represents a compelling strategy for enhancing anti-cancer efficacy.

Methods Based on the in-house screened anti-CLDN18.2 VHH, we have developed a novel tri-specific T cell engager targeting CLDN18.2 for gastric and pancreatic cancer immunotherapy. This tri-specific antibody was designed with binding to CLDN18.2, human serum albumin (HSA) and CD3 on T cells.

Results The DR30318 demonstrated binding affinity to CLDN18.2, HSA and CD3, and exhibited T cell-dependent cellular cytotoxicity (TDCC) activity in vitro. Pharmacokinetic analysis revealed a half-life of 22.2–28.6 h in rodents and 41.8 h in cynomolgus monkeys, respectively. The administration of DR30318 resulted in a slight increase in the levels of IL-6 and C-reactive protein (CRP) in cynomolgus monkeys. Furthermore, after incubation with human PBMCs and CLDN18.2 expressing cells, DR30318 induced TDCC activity and the production of interleukin-6 (IL-6) and interferon-gamma (IFN-γ). Notably, DR30318 demonstrated significant tumor suppression effects on gastric cancer xenograft models NUGC4/hCLDN18.2 and pancreatic cancer xenograft model BxPC3/hCLDN18.2 without affecting the body weight of mice.

Keywords Claudin 18.2 · T cell engager · Gastric cancer · Pancreatic cancer · Cytokines · TDCC

Introduction

Gastric cancer, ranked as the sixth most prevalent cancer globally, is the third leading cause of cancer-related mortality [1], and is widely recognized as one of the most challenging malignancies to treat. Although early gastric cancer exhibits a 5-year overall survival rate (OSR) exceeding 90% in Asia [2–5], the OSR for advanced gastric cancer remains low due to late-stage diagnosis in over 80% of patients [6]. Pancreatic cancer is characterized by a dismal prognosis and high mortality, making it the most lethal disease. In 2019, the survival rate of patients diagnosed with pancreatic adenocarcinoma was 24% at 1 year and only 9% at 5 years in the USA and Europe in 2019 [1, 7]. The relatively low survival rate can be partly attributed to the prevalence of advanced-stage diagnosis in most cases, as only approximately 20% of patients are diagnosed at an early stage when surgical resection is feasible [8]. Furthermore, even after surgery without additional therapy, more than 90% of patients experience disease relapse and succumb to their illness [9].

Zhe Ma and Zhenxing Zhou have contributed equally to the work.

✉ Yanshan Huang
yanshanhuang@doerbio.com

✉ Lushan Yu
yuls@zju.edu.cn

1 Institute of Drug Metabolism and Pharmaceutical Analysis, College of Pharmaceutical Sciences, Zhejiang University, Hangzhou 310058, Zhejiang Province, China

2 Department of Innovative Drug Discovery and Development, Zhejiang Doer Biologics Co., Ltd., Hangzhou 310058, Zhejiang Province, China

3 National Key Laboratory of Advanced Drug Delivery and Release Systems, Zhejiang University, Hangzhou 310058, China

4 Department of Pharmacy, Second Affiliated Hospital, School of Medicine, Zhejiang University, Hangzhou 310009, China

5 Jinhua Institute of Zhejiang University, Jinhua 321036, China

6 Department of Pharmacy, Shaoxing People's Hospital (Shaoxing Hospital, Zhejiang University School of Medicine), Shaoxing 312000, China

Currently, the market for gastric cancer immunotherapy is limited to HER2-targeted drugs [10–12], anti-PD-(L)1 agents [13, 14] and anti-VEGFR treatments [15]. However, these therapies have shown only modest benefits in gastric/GEJ cancer patients, with objective response rates (ORR) ranging between 3 and 11% [14, 16]. For pancreatic cancer, although monoclonal antibodies targeting integrin α3, Mucins, EGFR, TROP2 and α6β4 have demonstrated efficacy in pancreatic tumor xenograft models, their clinical translation has been limited with minimal survival benefits observed in patients [17–19]. Therefore, to address the unmet need for effective antibody-based therapies in gastric and pancreatic cancer treatment, the identification of a novel promising target is imperative.

Claudin 18 (CLDN18) is a member of the Claudin family with four transmembrane domains and has two splice variants, CLDN18.1 and CLDN18.2. In normal tissues, CLDN18.1 is strictly expressed on epithelial cells of lung tissue, while CLDN18.2 is exclusively expressed on differentiated gastric mucosal cells [20]. Notably, CLDN18.2 exhibits significantly aberrant expression in multiple cancers, such as gastric cancer [21–23], pancreatic cancer [24] and esophageal adenocarcinomas [25]. Given its specific expression pattern, targeting CLDN18.2 holds great promise for therapeutic interventions against gastric and pancreatic cancer. Zolbetuximab (IMAB362), which exerts potent antitumor activity through antibody-dependent cytotoxicity (ADCC) and complement-dependent cytotoxicity (CDC), is the world's first monoclonal antibody drug targeting CLDN18.2 [26]. In 2023, Astellas reported the exceptional efficacy of Zolbetuximab in phase III clinical trials for advanced unresectable or metastatic gastric or gastroesophageal junction (mG/GEJ) adenocarcinoma patients, particularly among Asian populations [27–29]. Meanwhile, various therapeutic modalities targeting CLDN18.2 are currently under investigation, including monoclonal antibody [30], bispecific antibody [31], CAR-T cell therapy and other approaches [32].

The bispecific T cell engager (BiTE) specifically targets the tumor cell antigen and CD3 on T cells, thereby inducing the potent T cell-dependent cellular cytotoxicity (TDCC). However, in terms of canonical BiTE, continuous intravenous infusion is needed to maintain therapeutic concentration due to its rapid clearance [33]. The antibody isotype immunoglobulin G (IgG) and human serum albumin (HSA) have longer plasma half-life of about 3 weeks in human body [34]. Strategies, based on IgG-Fc backbone or affinity reagents that recognize and bind HSA, can be used to extend the half-life of BiTE [35–37]. AMG910 is the first bispecific T cell engager targeting CLDN18.2 based on Amgen's half-extended (HLE) BiTE platform. A phase I clinical trial investigating AMG910 for patients with CLDN18.2 positive cancers is underway [38]. In this study, we developed a trispecific T cell engager DR30318 based on the MultipleBody® platform of Doer Biologics, specifically targeting CLDN18.2, HSA and CD3. The in vitro and in vivo studies demonstrated that DR30318 exhibited potent TDCC activity and robust efficacy in suppressing tumor growth. Pharmacokinetic (PK) studies revealed a linear PK profile in cynomolgus monkeys. The lower degree of cytokine release and robust tumor regression activity position DR30318 as a promising therapeutic agent for CLDN18.2 positive cancers.

Materials and methods

Cell lines

CHO-K1Q cells were cultured in CD02 medium (Quacell), BxPC3 and HEK293 cells were cultured in high glucose DMEM medium (BasalMedia) supplied with 10% fetal bovine serum (FBS, ExcellBio), Panc1, NUGC4 and SNU620 cells were cultured in RPMI 1640 medium (BasalMedia) supplied with 10% FBS.

For construction of CLDN18.2 over-expressing cells, the cDNA under the control of CMV promoter was cloned into the plasmid pDR05 or pBX to obtain the plasmids pDR05-CLDN18.2 and pBX-CLDN18.2, respectively. CHO-C18.2-gfpx cells were obtained by electroporation with pDR05-CLDN18.2, and under the selection of glutamine synthetase (GS)-based system. Panc1-C18.2, NUGC4-C18.2 and SNU620-C18.2 cells were obtained by transfection with Lipo3000 (Thermofisher) and selected under the pressure of puromycin (Invivogen).

Generation of DR30318

DR30318 is consisting of an in-house screened anti-CLDN18.2 variable domains of heavy chain of heavy-chain antibodies (VHH) from an *alpaca*, an anti-HSA nanobody and an anti-CD3 single-chain fragment variable (scFv). The gene sequence encoding DR30318 was cloned into the pDR03 vector to obtain the expression plasmid. Subsequently, transient transfection of HEK293 cells with pDR03-30318 was performed using PEI as a transfection reagent. The cultural supernatant containing DR30318 protein was collected and subjected to purification through affinity chromatography (Bestchrom Biosciences, AT Protein A Diamond). The purified protein underwent preliminary verification by SDS-PAGE (about 52 kDa) and Size Exclusion Chromatography 300 A (Agilent). Meanwhile, the benchmark AMG910 analog was expressed based on the sequence information released by Amgen (US11692031B2).

In vitro binding assay

The binding affinity of DR30318 to CLDN18.2 or CD3 was assessed using flow cytometry (FCM) method. CHO-CLDN18.2-gfpx cells (exogenously over-expressing the CLDN18.2 protein) or Jurkat cells were harvested and adjusted to 5 million cells/ml with assay buffer (RPMI 1640 supplemented with 1% FBS). The cell suspension was seeded into a round-bottomed 96-well plate, and serially diluted DR30318 was added and incubated for one hour at 4 °C. After two washes with PBS, the cells were further incubated with rabbit anti-VHH polyclonal antibody and fluorescent secondary antibody before being rewashed with PBS. Finally, the cell suspension was analyzed using a NovoCyte flow cytometer (Agilent, 2060R).

The binding affinity of DR30318 to serum albumin of human (HSA) and bovine (BSA) was determined using an enzyme-linked immunosorbent assay (ELISA). Briefly, HSA or BSA was immobilized onto 96-well microplates for the capture of DR30318. Subsequently, anti-VHH rabbit polyclonal antibody and HRP-labeled secondary antibody were sequentially incubated. Following five washes with PBST, TMB substrate was added and incubated, and the optical density at 450 nm (OD_{450}) was measured using a microplate reader.

TDCC reporter assay

An in vitro TDCC reporter assay was conducted to evaluate the antitumor activity of DR30318. Jurkat-NFAT-luc2p-10F2 (effector cells) and CLDN18.2 expression cells (target cells) such as CHO-C18.2-gfpx, BxPC3, Panc1, Panc1-C18.2, SNU620, SNU620-C18.2 and NUGC4-C18.2 were harvested, adjusted to 2.4×10^6/ml and 6×10^5/ml, respectively, and mixed at a ratio of 1:1 by volume. The mixture was seeded into a 96-well plate with 50 µl/well, followed by the addition of serially diluted DR30318 or other reference proteins at a volume of 50 µl/well. After incubation for 18 h at 37 °C, cell cultures were measured using the Bright-Glo™ Luciferase Assay System (Promega, E2620), according to the manufacturer's instructions.

PBMC-based TDCC assay

The antitumor activity of DR30318 was also assessed in vitro using the PBMC-based TDCC assay. T cells isolated using the Invitrogen™ MagniSort™ Human T cell Enrichment Kit (Invitrogen, 8804-6810-74) or the peripheral blood mononuclear cells (PBMCs) of two healthy donors and target cells BxPC3, Panc1, Panc1-C18.2, SNU620, SNU620-C18.2 and NUGC4-C18.2 were harvested and adjusted to 4×10^6/ml and 1×10^5/ml, respectively, and mixed at a ratio of 1:1 by volume. The mixture was seeded into a 96-well plate with 50 µl/well, followed by the addition of serially diluted DR30318 or other reference proteins at a volume of 50 µl/well. The cell culture plates were further incubated for 24 h at 37 °C. Then, the lactate dehydrogenase (LDH) levels in the supernatant were measured according to the instructions provided with the Cytotoxicity LDH Assay Kit (Donjido, CK12).

T cell stimulation assay

PBMCs of two healthy donors were seeded into 96-well U type plate and incubate with DR30318 or AMG910 analog for 0,3 or 7 days. Then, Alexa Fluor® 488 anti-Human CD3 (Biolegend, 317,310), PerCP anti-human CD8 (Biolegend, 344,708) and APC anti-human CD4 (Biolegend, 300,514) were applied for measurement of the BiTE—induced T cell proliferation.

Pharmacokinetics

The pharmacokinetic (PK) profiles of DR30318 were evaluated in rodents and non-human primates.

C57BL/6 and NOD-SCID mice (four females and four males), aged 6–7 weeks, received a tail intravenous infusion of DR30318 at doses of either 0.1 or 1 mg/kg. Blood samples were collected before and after administration at 1, 6, 24, 30, 48, 72, 96 and 120 h.

Cynomolgus monkeys (one female and one male per group) were intravenously infused with DR30318 at 0.03, 0.6 or 3 mg/kg. Blood samples were collected before administration, immediately after administration, at 4, 8, 24, 48, 72, 120 and 168 h. For repeat-dosage of DR30318, cynomolgus monkeys (two females and two males) were given 0.03 mg/kg DR30318 once a week. Blood samples were collected before and immediately after administration, as well as at 4, 8, 24-, 48-, 72- and 120-h post-dosage for both the first and fourth administrations.

The serum concentration of DR30138 was determined with the ELISA method.

Cytokines release

The serum samples from the 0.03 mg/kg and 3 mg/kg groups were analyzed for IL-2, IL-6, TNF-α and CRP.

To assess the potential risk of cytokines release syndrome (CRS) induced by DR30318 administration in the human study, the TDCC-based in vitro cytokine release assay was performed. In brief, CHO-C18.2-gfpx cells were used as target cells, and the PBMCs from two

healthy donors were used as effector cells. 4×10^4 cells of the target were incubated with 2×10^5 cells of the effector and serially gradient concentration of DR30318. After being incubated at 37 °C and 5% CO_2 for 24 h and 48 h, the culture plates were centrifugated at 1500 RPM for 5 min. The production of IL-2, IL-6, IL-10, TNF-α and IFN-γ in the supernatants was detected with LEGENDplex™ HU Th1 Panel (Biolegend, 741036).

Xenograft tumor models

To establish the human gastric cancer or pancreatic cancer model, male NCG mice (GemPharmatech), aged 6–8 weeks, were subcutaneously injected with 5×10^6 cells of gastric cancer cell line NUGC4/hCLDN18.2 or pancreatic cancer cell line BxPC3/hCLDN18.2. After 7 days, 2×10^6 PBMC cells were intravenously infused via tail injection. Upon reaching an average tumor volume of approximately 40–60 mm^3, the mice were randomly allocated into five groups, each group containing six mice, for intraperitoneal administration of DR30318: a vehicle control group receiving normal saline, BIW (twice a week) at doses of 0.03 mg/kg and 0.1 mg/kg, respectively, and QD (daily) at doses of 0.03 mg/kg and 0.1 mg/kg, respectively.

Tumor volume was measured twice weekly with a Vernier caliper and determined according to the following equation: Tumor volume (mm^3) = 1/2 length × $width^2$. After the mice were sacrificed, the tumors were dissected and photographed.

Immunohistochemical staining

Tumor tissues from Xenograft tumor models were collected, fixed, paraffin-embedded and sectioned. The sections were floated onto clean glass slides, deparaffinized and antigen retrieval with microwave. The endogenous peroxidase activity was then blocked at room temperature by a 5–10 min incubation in the final developmental 3% H_2O_2 before being blocked with normal goat serum. The slides were then incubated with anti-Claudin 18 [34H14L15] antibody (abcam, ab203563) or anti-CD3 epsilon antibody (abcam, ab5690). Finally, the slides were counterstained with hematoxylin and recorded by Nikon microscope.

Statistical analysis

All statistical analyses were conducted using the GraphPad Prism software. Experimental data were presented as mean ± standard deviation (SD) or mean ± standard error of the mean (SEM). Two-group comparisons were assessed using the student's *t* test. A value of $p < 0.05$ was considered statistically significant.

Results

DR30318 is a tri-specific fusion protein engineered to specifically target CLDN18.2, human serum albumin and CD3

Previously, we have isolated multiple anti-CLDN18.2 variable domains of heavy chain of heavy-chain antibodies (VHH) from an *alpaca* [35]. Utilizing the optimal VHH sequence, we successfully engineered DR30318 as a T cell engager with specific binding to CLDN18.2, HSA and CD3. As depicted in Fig. 1A, DR30318 is a 52.3 kDa molecule composed of an N-terminal anti-CLDN18.2 VHH domain, a C-terminal anti-CD3 scFv domain and an anti-HSA domain which is designed to enhance its in vivo half-life. The three binding domains monovalent bind to targets, respectively, and were connected via G_4S linkers. The binding affinities of DR30318 to human CLDN18.2 and human CD3 were determined using flow cytometry, resulting in EC_{50} values of 14.4 nM and 3.14 nM (Fig. 1B, C), respectively. DR30318 exhibited strong affinity toward HSA with an EC_{50} value of 0.44 nM and no significant binding was observed with BSA (Fig. 1D).

DR30318 exhibits potent TDCC activity in vitro

Firstly, a luciferase reporter gene assay was employed to evaluate the TDCC activity of DR30318. Utilizing CHO-CLDN18.2-gfpx cells as target cells and Jurkat-NFAT-Luc cells as effectors, both DR30318 and AMG910 exhibited robust TDCC activities (Figure S1 in Supplementary materials II), with EC_{50} values of 0.047 nM and 0.062 nM, respectively. The isotype control, which binds to HSA and CD3 but not to CLDN18.2, exhibited no TDCC activity. Meanwhile, DR30318 did not show TDCC activity against CHO-K1Q and HEK293 cells which have no endogenous CLDN18.2 expression (Figure S2 in Supplementary materials II), thereby indicating a CLDN18.2 specific mechanism of action for DR30318. Gastric cancer cell lines SNU620, SNU620-C18.2, NUGC4-C18.2 and pancreatic cancer cell lines BxPC3, Panc1, Panc1-C18.2, which endogenously or stable exogenously transfection express CLDN18.2 (Figure S3 in Supplementary materials II), were utilized as the target cells. Against both gastric (Fig. 2A) and pancreatic cancer (Fig. 2B) cell lines, DR30318 was more potential especially against low or moderate CLDN18.2 expressing cells.

Additionally, a PBMC-based TDCC assay was performed to evaluate the TDCC activity of DR30318. PBMCs obtained from two healthy volunteers were employed as the effector cells. Against both gastric

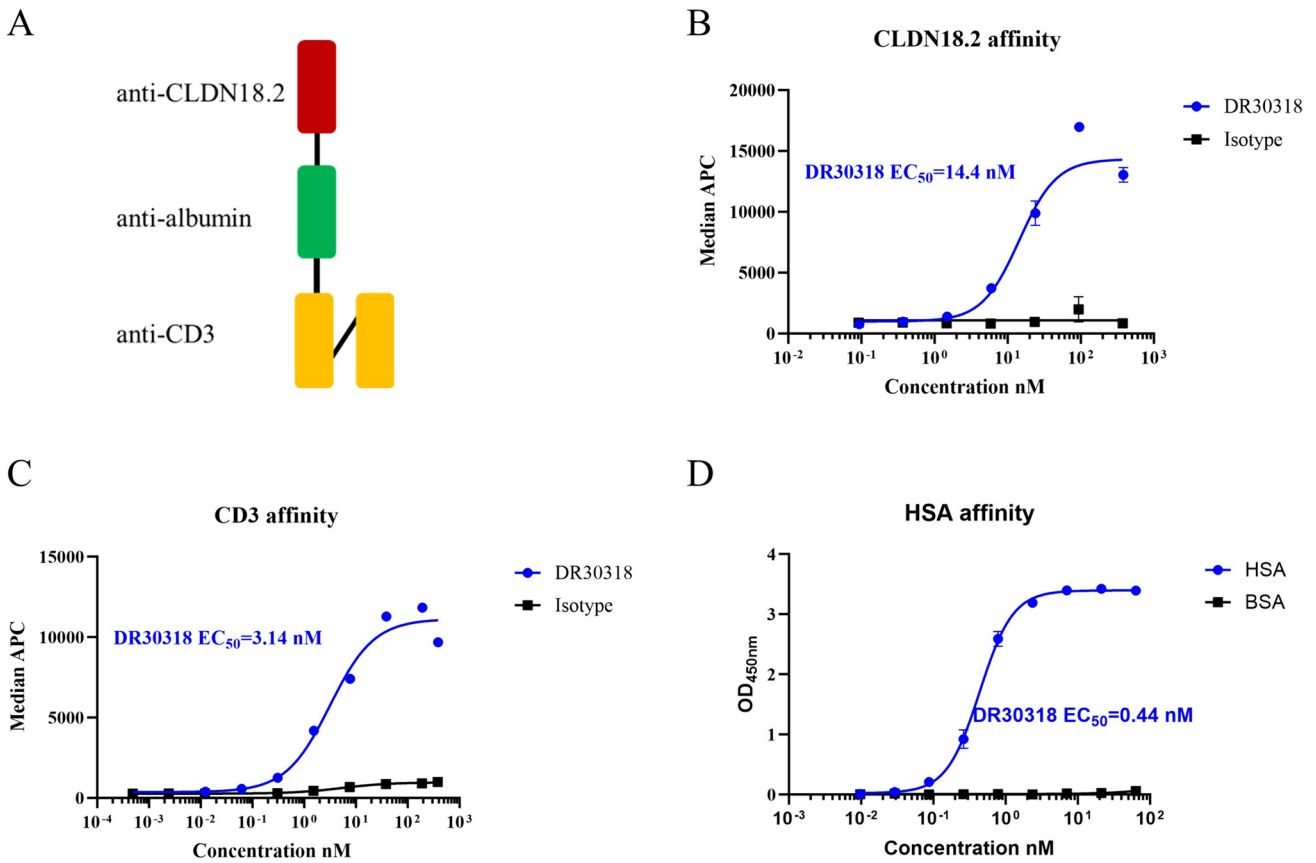

Fig. 1 The structure and binding affinities of DR30318 in vitro. **A** Schematic diagram of DR30318 structure. DR30318 consists of an anti-CLDN18.2 domain (red), an anti-CD3 scFv domain (orange), an HSA binding domain (green) and two G_4S linkers (black). **B** Binding affinity of DR30318 to human CLDN18.2. Serial dilutions of DR30318 (blue) and isotype control (black) were incubated with CHO-CLDN18.2-gfpx cells (over-expressing CLDN18.2) and detected by flow cytometry. The isotype control, structurally similar to DR30318, binds to HSA and CD3 but not to CLDN18.2. **C** Binding affinity of DR30318 to CD3. Serial dilutions of DR30318 (blue) and isotype control (black) were incubated with Jurkat (endogenously expressing CD3) and detected by flow cytometry. **D** Binding of DR30318 to HSA. Serial dilutions of DR30318 were incubated with plate-bound HSA (blue) or BSA (black) and detected using ELISA

(Fig. 3A) and pancreatic cancer (Fig. 3B) cell lines, DR30318 shows better TDCC potential especially against low or moderate CLDN18.2 expressing cells. After being incubated with equimolar protein, less cancer cells in DR30318 treatment group showed good stretched state (Figure S4 in Supplementary materials II). These data indicated the promising TDCC activity of DR30318 and the need for in vivo assessment.

DR30318 enhances T cell proliferation in vitro

After being incubated for 3 or 7 days, the proportion of $CD3^+$ T cells slightly increased when treated with DR30318 compared to those treated with AMG910. However, there was no significant difference observed in the levels of $CD4^+$ and $CD8^+$ T cells between incubation with DR30318 and AMG910 (Fig. 4).

DR30318 pharmacokinetic profiles in rodents and non-human primate

The pharmacokinetic profiles of DR30318 were first evaluated in vivo in both rodents (Fig. 5A) and non-human primates (Fig. 5B). Following single intravenous administration of doses at 0.1 and 1 mg/kg, DR30318 exhibited nonlinear pharmacokinetics in C57BL/6 mice with a half-life of 28.6 ± 0.3 h, and the drug exposure ratio was lower than the dose ratio (Table 1). However, in NOD/SCID mice which lacks immune cell, DR30318 demonstrated nearly linear pharmacokinetics with a half-life of 22.2 ± 2.3 h. These results provided the basis for dosage design in pharmacodynamics studies.

After intravenous administration of 0.03, 0.6 and 3 mg/kg, DR30318 exhibited linear pharmacokinetics in cynomolgus monkeys (Fig. 5B and Table 2), with a half-life of 41.8 ± 8.7 h. No significant sex-related differences were observed, as evidenced by the exposure ratio of C_{max} and

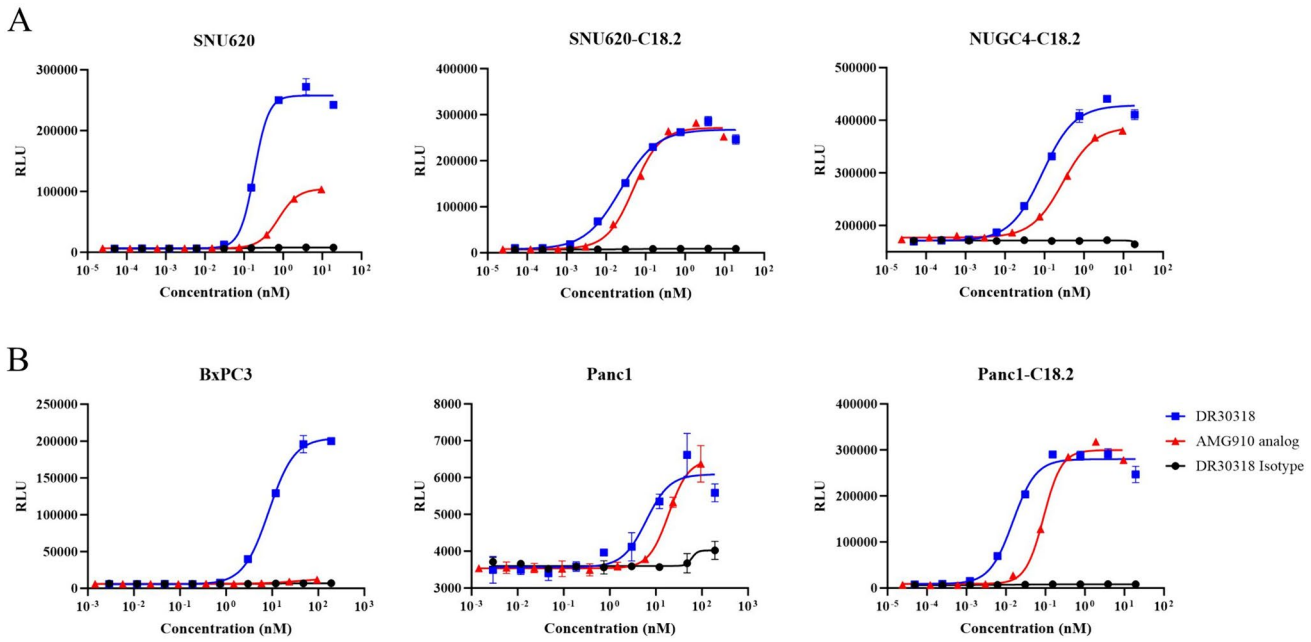

Fig. 2 TDCC activities of DR30318 and AMG910 determined by the luciferase-based reporter gene assay. **A** Serial dilutions of DR30318 (blue), AMG910 (red) and isotype control (black) were incubated with CLDN18.2 expression gastric cancer cells (target cells) and Jurkat-NFAT-Luc (effector cells). **B** Serial dilutions of DR30318 (blue), AMG910 (red) and isotype control (black) were incubated with CLDN18.2 expression pancreatic cancer cells (target cells) and Jurkat-NFAT-Luc (effector cells)

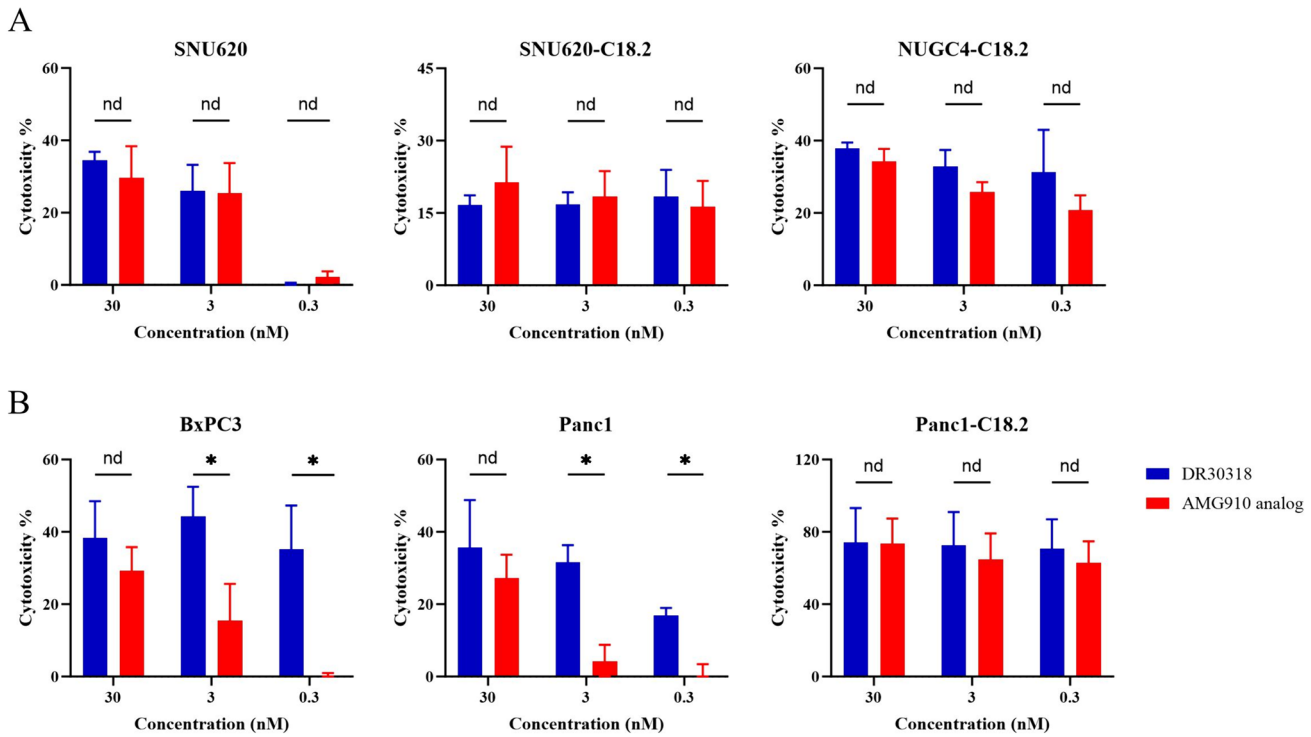

Fig. 3 TDCC activities of DR30318 and AMG910 determined by the PBMC-based TDCC assay. **A** Serial dilutions of DR30318 (blue), AMG910 (red) and isotype control (black) were incubated with CLDN18.2 expression gastric cancer cells (target cells) and T cells isolated from PBMC (SNU620) or PBMCs (SNU620-C18.2 and NUGC4-C18.2) of two healthy donors (effector cells). **B** Serial dilutions of DR30318 (blue), AMG910 (red) and isotype control (black) were incubated with CLDN18.2 expression pancreatic cancer cells (target cells) and PBMCs of two healthy donors (effector cells). * indicated a significant difference of $p < 0.05$

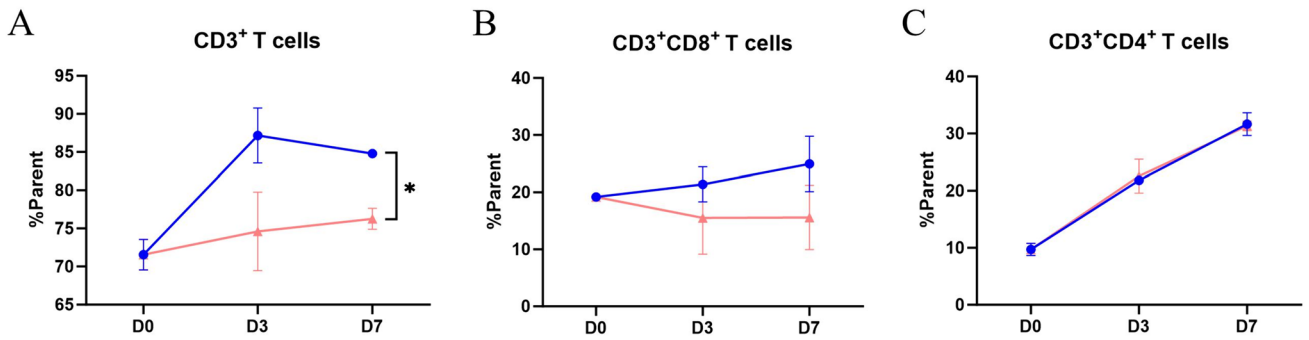

Fig. 4 The T cell stimulation effect of DR30318 in vitro. PBMCs of 2 healthy donors were seeded into 96-well U type plate and being incubated with DR30318 (blue) and AMG910 (red) for 0, 3 and 7 days. $CD3^+$ T cells (**A**), $CD3^+$ $CD8^+$ T cells (**B**) and $CD3^+$ $CD4^+$ T cells (**C**) were stained and analyzed with NovoCyto 2060R (Aligent). * indicated a significant difference of $p < 0.05$ at day 7

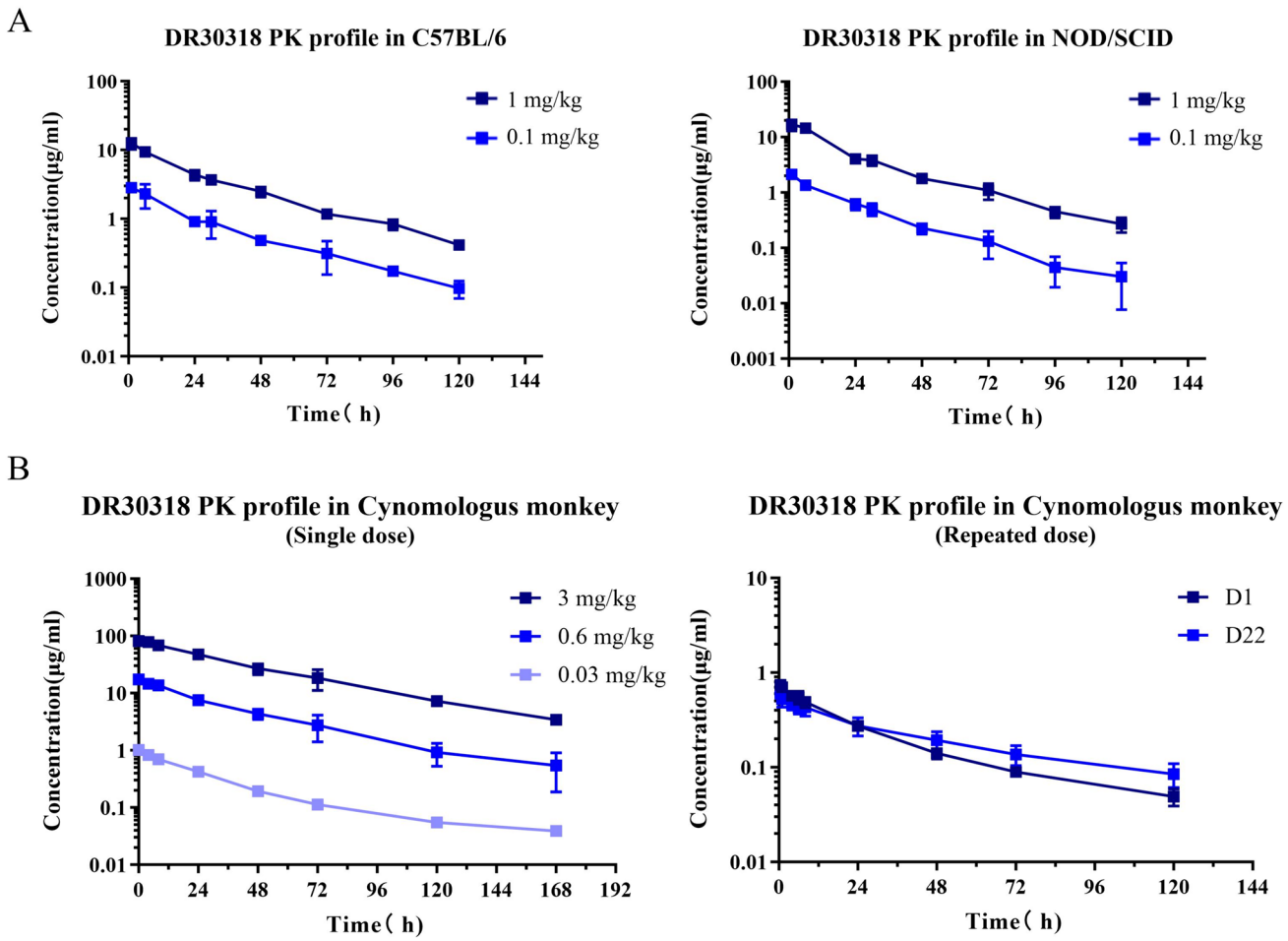

Fig. 5 The pharmacokinetic profiles of DR30318 in vitro. **A** The pharmacokinetic profiles of DR30318 in C57BL/6 mice. After the single dose administration of DR30318 at 0.1 mg/kg (blue) or 1 mg/kg (dark blue), the serum concentrations were determined at specified time points using ELISA. **B** The pharmacokinetic profiles of DR30318 in NOD/SCID mice. After the single dose administration of DR30318 at 0.1 mg/kg (blue) or 1 mg/kg (dark blue), the serum concentrations were determined at specified time points using ELISA. **C** The pharmacokinetic profiles of DR30318 after a single dose administration in cynomolgus monkeys. After the administration of a single dose of DR30318 at 0.03 mg/kg (light blue), 0.6 mg/kg (blue) or 3 mg/kg (dark blue), serum concentrations were determined at specified time points using ELISA. **D**. The pharmacokinetic profiles of DR30318 after a repeat dose administration in cynomolgus monkeys. After four cycles of repeated administration of DR30318 at 0.03 mg/kg, serum concentrations were determined at specified time intervals using ELISA

Table 1 Pharmacokinetic parameters of DR30318 in rodents

Parameter*	Unit	C57BL/6		NOD-SCID	
		0.1 mg/kg ($n=8$)	1 mg/kg ($n=8$)	0.1 mg/kg ($n=8$)	1 mg/kg ($n=8$)
$t_{1/2}$	h	28.40	28.81	20.53	23.85
C_{max}	μg/ml	2.83	12.70	2.12	17.06
AUC_{0-t}	μg/ml*h	81.15	355.30	45.96	399.19
$AUC_{0-\infty}$	μg/ml*h	85.13	372.60	46.86	408.46
Vz	mL/kg	48.13	111.55	63.22	84.23
CL	mL/(h·kg)	1.17	2.68	2.13	2.45
$MRT_{0-\infty}$	h	34.85	35.30	25.55	24.85
Dose ratio		1 : 10		1 : 10	
C_{max} ratio		1 : 4.5		1 : 8.1	
AUC_{0-t} ratio		1 : 4.4		1 : 8.7	
$AUC_{0-\infty}$ ratio		1 : 4.4		1 : 8.7	

*The PK parameters were derived from the mean concentration at each time point

AUC being close to 1.0. The accumulation of DR30318 was not evident after 4-week doses of DR3018 (Table 1 in Supplementary materials I).

Cytokines release assay of DR30318

Cytokine release syndrome (CRS) frequently occurs after immunotherapy treatment that activates T cells, particularly when employing the T cell engager drug format. Therefore, in the PK study and an in vitro PBMC stimulation assay, we assessed the cytokine release induced by DR30318 administration.

The serum samples from the PK study of 0.03 mg/kg and 3 mg/kg groups were analyzed for the production of cytokines. As depicted in Fig. 6A and Table 2 in Supplementary materials I, DR30318 elicited a transient elevation of IL-6 levels at the third hour in the 0.03 mg/kg group or at the seventh hour in the 3 mg/kg group, which subsequently returned to baseline by 24 h. The administration of DR30318 at a dosage of 0.03 mg/kg resulted in a slight increase in IL-2 levels between the third- and seventh-hour post-administration. However, continuous elevation of CRP was observed following DR30318 administration, while no production of TNF-α was detected.

Furthermore, DR30318 was incubated with human PBMCs from two healthy donors in the presence or absence of target cells to assess the potential risk of CRS. As depicted in Fig. 6B and Table 3 in Supplementary materials I, DR30318 elicited robust production of IL-6 and IFN-γ as well as trace amounts of IL-2, IL-10 and TNF-α when CHO-CLDN18.2-gfpx target cells were present. Conversely, without target cells, DR30318 did not induce significant cytokine production.

DR30318 treatment induces tumor regression in xenograft models

PBMC-based humanized xenograft models were utilized to investigate the tumor growth inhibitory effects of DR30318. The CLDN18.2 expression of the xenograft models was measured using immunohistochemical staining method, also was the CD3 positive cell in the tumor tissues. In our previous study, the CD3 positive rate in anti-CD3 scFv fusion protein treatment group showed no significant increase compared with vehicle group (data not shown), though the T cell stimulation assay using PBMCs from healthy donors showed that DR30318 could promote $CD3^+$ T cell proliferation (Fig. 4A), so we monitored the tumor-infiltrating CD3 T cells at the final of study instead of dynamic comparison.

In the gastric cancer NUGC4/hCLDN18.2 PBMC humanized tumor model, DR30318 demonstrated potent tumor inhibitory efficacy (Fig. 7A). In the QD dosing group, complete regression of tumors was observed with DR30318 at the end of the study. Furthermore, in the BIW dosing group, administration of 0.03 mg/kg and 0.1 mg/kg of DR30318 exhibited potent tumor inhibition efficacy, resulting in complete tumor remission in five out of six mice and significant tumor regression in all six mice (Fig. 7C). The body weight did not show any significant differences among the five groups (Fig. 7B), indicating that DR30318 holds promise as a safe and effective therapeutic candidate for gastric cancer treatment.

In the pancreatic cancer BxPC3/hCLDN18.2 PBMC humanized tumor model, DR30318 demonstrated a significant antitumor effect (Fig. 8A). From day 20 to day 34, there was an observed dose-dependent and frequency-dependent inhibitory effect on tumor growth. By the end of the study on Day 34, DR30318 nearly achieved complete regression of tumors in all treatment groups (Fig. 8C). Meanwhile, the administration of DR30318 did not elicit any detrimental

Table 2 Pharmacokinetic parameters of DR30318 in Cynomolgus macaques

Parameter	Unit	0.03 mg/kg		0.6 mg/kg		3 mg/kg	
		Male ($n=1$)	Female ($n=1$)	Male ($n=1$)	Female ($n=1$)	Male ($n=1$)	Female ($n=1$)
$t_{1/2}$	h	34.54	57.65	36.62	38.15	45.87	37.73
C_{max}	μg/ml	1.04	1.00	16.87	17.78	82.73	79.28
AUC_{0-t}	μg/ml*h	33.03	33.16	569.18	714.36	3494.02	4198.06
$AUC_{0-\infty}$	μg/ml*h	35.17	36.07	584.66	758.33	3699.57	4404.15
Vz	mL/kg	42.50	69.18	54.22	43.55	53.66	37.08
CL	mL/(h·kg)	0.85	0.83	1.03	0.79	0.81	0.68
$MRT_{0-\infty}$	h	48.10	56.26	37.84	53.24	50.65	53.16
Dose ratio		1 : 20.0 : 100.0					
C_{max} ratio		1 : 17.0 : 79.4					
AUC_{0-t} ratio		1 : 19.4 : 116.0					
$AUC_{0-\infty}$ Ratio		1 : 18.9 : 113.8					

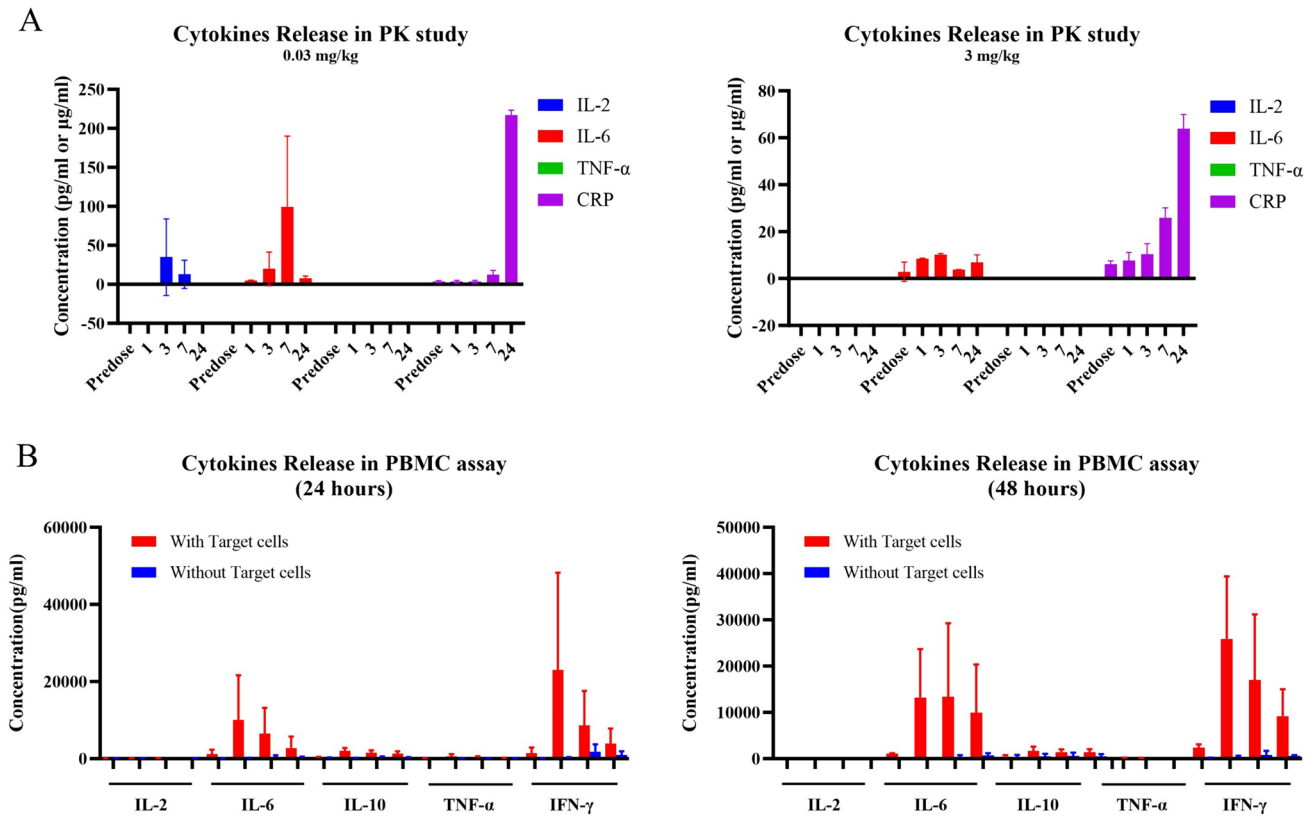

Fig. 6 Cytokines release induced by DR30318. **A** Cytokines in PK samples of 0.03 mg/kg group. PK samples were collected at predose, 1 h, 3 h, 7 h and 24 h time points and analyzed for the levels of IL-2 (blue histogram), IL-6 (red histogram), TNF-α (green histogram) and CRP (violet histogram). Data are displayed with Mean ± SD ($n=3$). The concentration of IL-2, IL-6 and TNF-α was demonstrated in pg/ml and CRP in μg/ml. **B** Cytokines in PK samples of 3.0 mg/kg group. PK samples were collected at predose, 1 h, 3 h, 7 h and 24 h time points and analyzed for the levels of IL-2 (blue histogram), IL-6 (red histogram), TNF-α (green histogram) and CRP (violet histogram). Data are displayed with Mean ± SD ($n=3$). The concentration of IL-2, IL-6 and TNF-α was demonstrated in pg/ml and CRP in μg/ml. **C** DR30318 was incubated with PBMC effector cells ($n=2$) and CHO-CLDN18.2-gfpx target cells at concentrations of 0, 0.025, 0.5 and 10 μg/ml for 24 h. The red histogram represents the presence of target cells, while the blue histogram represents their absence. The culture supernatant was collected, and the IL-2, IL-6, IL-10, TNF-α and IFN-γ levels were quantified. **D** DR30318 was incubated with PBMC effector cells ($n=2$) and CHO-CLDN18.2-gfpx target cells at 0, 0.025, 0.5 and 10 μg/ml concentrations for 48 h. The red histogram represents the presence of target cells, while the blue histogram represents their absence. The culture supernatant was collected, and the IL-2, IL-6, IL-10, TNF-α and IFN-γ levels were quantified

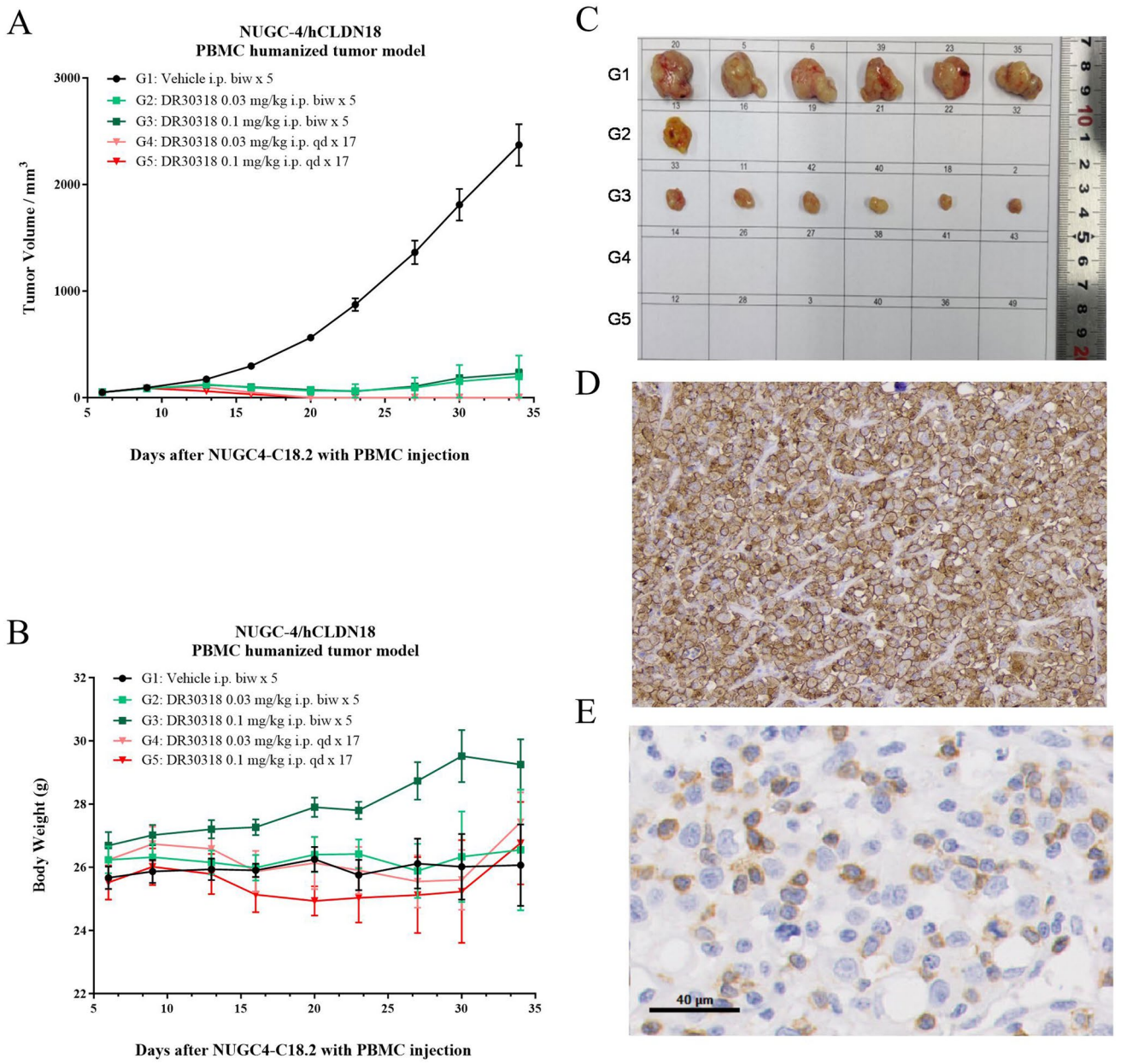

Fig. 7 Tumor growth inhibition of DR30318 in human gastric cancer xenograft model. **A** Tumor growth curves of NUGC4/hCLDN18.2 bearing mice injected with different formulations. **B** Body weight changes of NUGC4/hCLDN18.2 bearing mice injected with different formulations. Data are shown as mean ± SEM, $n = 6$, $^{***}p < 0.001$ (vs. Vehicle). **C** Representative tumor images treated with different formulations were captured at the study endpoint. **D** Representative image of CLDN18.2 expression in tumor of vehicle group at the study endpoint. **E** Representative image of CD3 expression in tumor of vehicle group at the study endpoint

impact on body weight across all experimental groups (Fig. 8B), thereby establishing DR30318 as a safe and productive therapeutic candidate for treating pancreatic cancer.

Discussion

Globally, gastric and pancreatic cancers rank among the most prevalent malignancies and are leading contributors to mortality in oncology [39, 40]. Due to the scarcity of effective early diagnosis, a considerable number of individuals are diagnosed with advanced or metastatic disease, resulting in a 5-year survival rate below 20% for gastric cancer and merely 2% for pancreatic cancer [41, 42]. With the induction

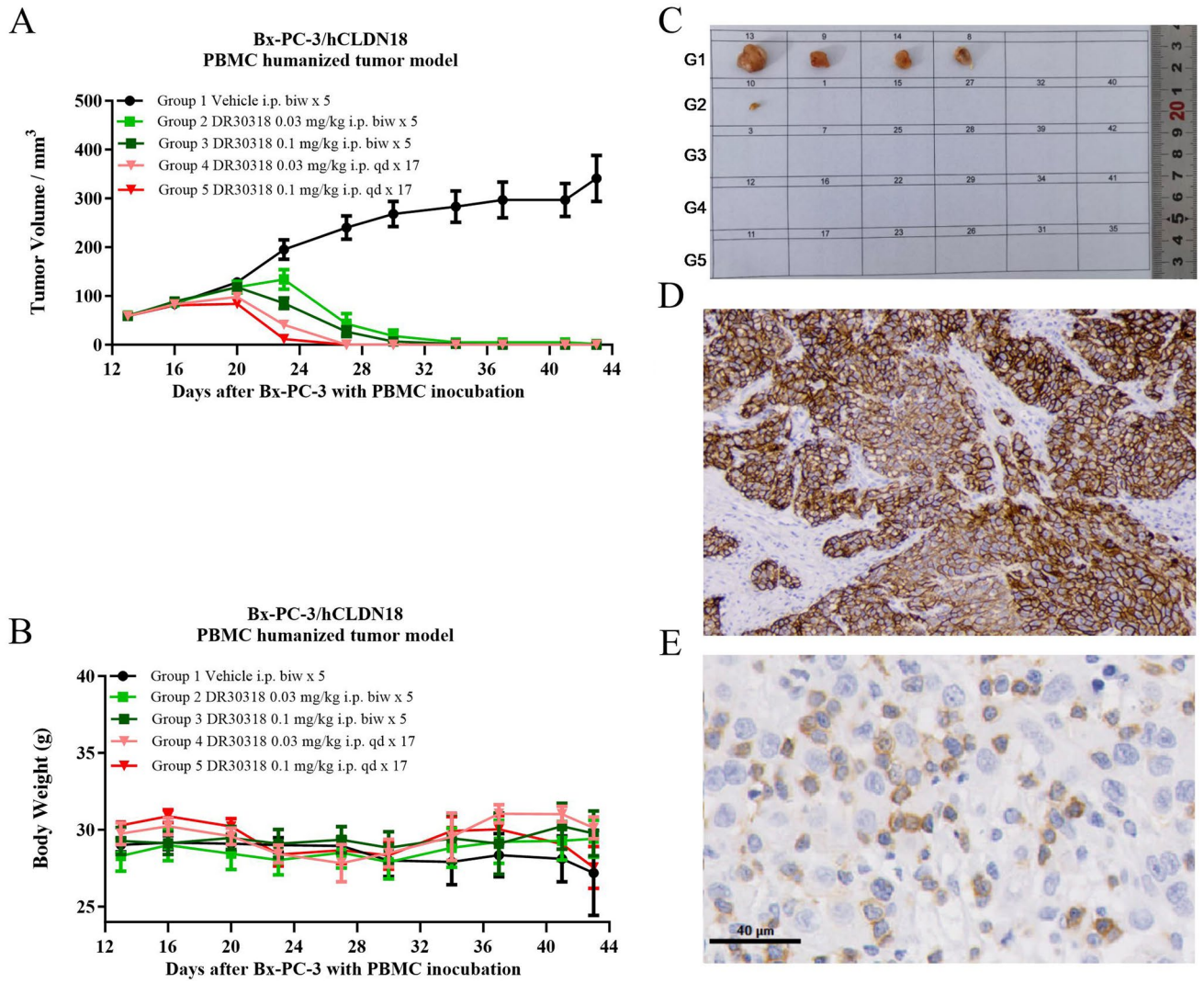

Fig. 8 Tumor growth inhibition of DR30318 in human pancreatic cancer xenograft model. **A** Tumor growth curves of BxPC3/hCLDN18.2 bearing mice injected with different formulations. **B** Body weight changes of BxPC3/hCLDN18.2 bearing mice injected with different formulations. Data are shown as mean ± SEM, $n = 6$, $^{***}p < 0.001$ (vs. Vehicle). **C** Representative tumor images treated with different formulations were captured at the study endpoint. **D** Representative image of CLDN18.2 expression in tumor of vehicle group at the study endpoint. **E** Representative image of CD3 expression in tumor of vehicle group at the study endpoint

of combination chemotherapy such as gemcitabine and nab-paclitaxel or FOLFIRINOX, the 5-year survival reached up to approximately 11% in 2021 [43], pancreatic cancer is still the most dismal disease. Consequently, substantial unmet clinical needs for both gastric and pancreatic cancers exist. CLDN18.2 demonstrates aberrant overexpression in various malignancies, including gastric and pancreatic cancer; however, its expression is strictly confined to gastric mucosal cells in healthy tissues, rendering it a promising therapeutic target for CLDN18.2 positive cancers.

The investigational Zolbetuximab, a first-in-class monoclonal antibody specifically targeting CLDN18.2, demonstrated promising results in Astellas's Phase III SPOTLIGHT trial. Combination therapy with Zolbetuximab and mFOLFOX6 resulted in a significant improvement in median progression-free survival (8.21 months VS 6.80 months) and a notable reduction in the risk of mortality (hazard ratio [HR] 0.75, 95% confidence interval [CI] 0.60–0.94) [44]. However, Zolbetuximab demonstrates efficacy exclusively in patients exhibiting robust CLDN18.2 expression (≥ 75% of tumor cells displaying moderate-to-strong membranous staining for CLDN18.2). Therefore, there remains an urgent need to explore novel therapeutic modalities targeting CLDN18.2 positive cancers.

T cell engagers (TCEs) hold great promise as a therapeutic modality, enabling the redirection of T cells toward specific tumor antigens. AMG910, developed on AMGEN's HLE platform, represents the pioneering clinical entry of

a CLDN18.2-targeting TCE [45]. In our study, we successfully developed a tri-specific TCE, DR30318, which exhibited simultaneous binding to CLDN18.2, HSA and CD3 in vitro affinity assays. This unique characteristic of DR30318 induced potent TDCC activity in vitro as demonstrated by both reporter gene TDCC assay and PBMC-based TDCC assay using T cells isolated from PBMC or PBMCs of healthy donors. Its potent TDCC effect against low or moderate CLDN18.2 expressing cells even in lower concentration made it exciting for the antigen degradation during course of disease or therapy. Moreover, the HSA binding domain (with serum albumin affinity from high to low: human ≈ cynomolgus monkey > mouse, data not shown) endowed DR30318 with a relatively longer half-life of 22.2–28.6 h in rodents and 41.8 h in cynomolgus monkey compared to canonical BiTE. Unlike most Fc-based TCEs, DR30318 is a monomeric fusion protein that possesses several appealing characteristics, including facile manufacturability and enhanced penetration into solid tumor tissues due to its low molecular weight.

Cytokine release syndrome (CRS) is a commonly observed adverse event in T cell engaging immunotherapies, particularly for TCEs, with IL-6 playing a pivotal role in the pathophysiology of CRS [46]. In the in vivo PK study conducted on cynomolgus monkeys, administration of DR30318 at doses of 0.03 mg/kg and 3 mg/kg resulted in a transient and slight increase in IL-6 production, which remained significantly lower than the level reported in certain publication [47]. The C-reactive protein (CRP) demonstrates a rapid response to IL-6 stimulation and can serve as a reliable biomarker for monitoring the progression of CRS [48]. In our study, administration of DR30318 resulted in a sustained elevation of CRP levels, potentially indicating an on-target off-tumor toxicity in the stomach, as evidenced by observed gastric-related adverse effects such as anorexia, nausea and mucosal damage (data not shown). However, DR30318 did not induce significant production of TNF-α and IL-2. In vitro coculture with human PBMCs demonstrated that DR30318 elicited potent TDCC activities and triggered the release of IL-6 and IFN-γ in the presence of target cells. Conversely, in the absence of target cells, DR30318 failed to induce cytokine production, thereby suggesting a mechanism of action dependent on binding to CLDN18.2 and minimizing the risk of peripheral immune system activation.

DR30318 demonstrated potent tumor growth inhibition in both gastric and pancreatic xenograft models. A daily dosage of 0.03 mg/kg in the gastric cancer model effectively suppressed tumor growth. In the pancreatic cancer model, treatment with DR30318 nearly resulted in complete tumor regression by the end of the study period. Significantly, administration of DR30318 did not adversely affect body weight in mice, indicating its safety profile and potential as a promising therapeutic candidate for gastric and pancreatic cancers. Considering that DR30318 induced only mild IL-6 production at 0.03 mg/kg and 3 mg/kg, it suggests a wide therapeutic window for DR30318, which is a crucial characteristic for most therapeutic compounds targeting TCEs.

In summary, we successfully constructed a tri-specific T cell engager, DR30318. In vitro and in vivo studies demonstrated CLDN18.2 target dependent TDCC activities to kill the tumor cells. The lower degree of cytokine release and robust tumor regression activity indicated that DR30318 was a promising therapeutic agent for CLDN18.2 positive cancers.

Supplementary Information The online version contains supplementary material available at https://doi.org/10.1007/s00262-024-03673-x.

Author contributions LY and YH conceived, designed and supervised the project. ZM and ZZ wrote the manuscript, designed and conducted experiments. WD, SS and SZ contributed to the in vivo studies. GY and XZ performed the protein expression and purification. CL, YL and FO conducted part of the in vitro experiments. MRD modified and edited the manuscript. All authors contributed to the article and approved the submitted version.

Funding This work was supported by the Ten-thousand Talents Program of Zhejiang Province (2021R52013) and grants from The National Natural Science Foundation of China (82274003, 81973390).

Declarations

Conflict of interest ZM, ZZ, WD, GY, SS, SZ, XZ, CL, YL and YH are current employees of Zhejiang Doer Biologics Corporation, Ltd. YH is a shareholder of Zhejiang Doer Biologics Corporation, Ltd. No other authors have a conflict of interest. We declare that the work presented here is free of any bias.

Ethical approval The experiments involving rodents and non-human primate related experiments were approved, conducted and supervised by the Institutional Animal Care and Use Committee (IACUC) in Yicon (Beijing) Biomedical Technology Inc.

References

1. Sung H, Ferlay J, Siegel RL et al (2021) Global cancer statistics 2020: GLOBOCAN estimates of incidence and mortality worldwide for 36 cancers in 185 countries. CA Cancer J Clin

71(3):209–249. https://doi.org/10.3322/caac.21660[publishedOnlineFirst:2021/02/05]
2. Sigon R, Canzonieri V, Cannizzaro R et al (1998) Early gastric cancer: diagnosis, surgical treatment and follow-up of 45 cases. Tumori 84(5):547–551. https://doi.org/10.1177/030089169808400507
3. Yang K, Lu L, Liu H et al (2021) A comprehensive update on early gastric cancer: defining terms, etiology, and alarming risk factors. Expert Rev Gastroenterol Hepatol 15(3):255–273. https://doi.org/10.1080/17474124.2021.1845140
4. Asaka M, Mabe K (2014) Strategies for eliminating death from gastric cancer in Japan. Proc Jpn Acad Ser B Phys Biol Sci 90(7):251–258. https://doi.org/10.2183/pjab.90.251
5. Wang X, Zhao J, Shen Z et al (2020) Multidisciplinary approach in improving survival outcome of early-stage gastric cancer. J Surg Res 255:285–296. https://doi.org/10.1016/j.jss.2020.05.058
6. Bonelli P, Borrelli A, Tuccillo FM et al (2019) Precision medicine in gastric cancer. World J Gastrointest Oncol 11(10):804–829. https://doi.org/10.4251/wjgo.v11.i10.804
7. Rawla P, Sunkara T, Gaduputi V (2019) Epidemiology of pancreatic cancer: global trends, etiology and risk factors. World J Oncol 10(1):10–27. https://doi.org/10.14740/wjon1166
8. Klein AP (2021) Pancreatic cancer epidemiology: understanding the role of lifestyle and inherited risk factors. Nat Rev Gastroenterol Hepatol 18(7):493–502. https://doi.org/10.1038/s41575-021-00457-x
9. Zhu H, Li T, Du Y et al (2018) Pancreatic cancer: challenges and opportunities. BMC Med 16(1):214. https://doi.org/10.1186/s12916-018-1215-3
10. Uchôa BCDM, Pirolli R, Siqueira LBMG, et al. (2021) HER2-low and gastric cancer: a prognostic biomarker? 2021;39(15_suppl):e16086-e86. https://doi.org/10.1200/JCO.2021.39.15_suppl.e16086
11. Bang YJ, Van Cutsem E, Feyereislova A et al (2010) Trastuzumab in combination with chemotherapy versus chemotherapy alone for treatment of HER2-positive advanced gastric or gastro-oesophageal junction cancer (ToGA): a phase 3, open-label, randomised controlled trial. Lancet 376(9742):687–697. https://doi.org/10.1016/s0140-6736(10)61121-x
12. Zhu Y, Zhu X, Wei X et al (2021) HER2-targeted therapies in gastric cancer. Biochim Biophys Acta 1876(1):188549. https://doi.org/10.1016/j.bbcan.2021.188549
13. Cao X, Zhang M, Li N et al (2023) First-line nivolumab plus chemotherapy versus chemotherapy alone for advanced gastric cancer, gastroesophageal junction cancer, and esophageal adenocarcinoma: a cost-effectiveness analysis. Ther Adv Med Oncol 15:17588359231171038. https://doi.org/10.1177/17588359231171038
14. Muro K, Fuchs CS, Jang RW-J, et al (2018) KEYNOTE-059 cohort 1: Pembrolizumab (Pembro) monotherapy in previously treated advanced gastric or gastroesophageal junction (G/GEJ) cancer in patients (Pts) with PD-L1+ tumors—Asian subgroup analysis. 36(4_suppl):723–23. https://doi.org/10.1200/JCO.2018.36.4_suppl.723
15. Patel TH, Cecchini M (2020) Targeted therapies in advanced gastric cancer. Curr Treat Options Oncol 21(9):70. https://doi.org/10.1007/s11864-020-00774-4
16. Chan JA, Blaszkowsky LS, Enzinger PC et al (2011) A multicenter phase II trial of single-agent cetuximab in advanced esophageal and gastric adenocarcinoma. Ann Oncol 22(6):1367–1373. https://doi.org/10.1093/annonc/mdq604
17. Arias-Pinilla GA, Modjtahedi H (2021) Application of monoclonal antibodies in pancreatic cancer: advances, challenges and future opportunities. Cancers (Basel). https://doi.org/10.3390/cancers13081781
18. Chandana S, Babiker HM, Mahadevan D (2019) Therapeutic trends in pancreatic ductal adenocarcinoma (PDAC). Expert Opin Investig Drugs 28(2):161–177. https://doi.org/10.1080/13543784.2019.1557145
19. Kaplon H, Crescioli S, Chenoweth A et al (2023) Antibodies to watch in 2023. MAbs 15(1):2153410. https://doi.org/10.1080/19420862.2022.2153410
20. Sahin U, Koslowski M, Dhaene K et al (2008) Claudin-18 splice variant 2 is a pan-cancer target suitable for therapeutic antibody development. Clin Cancer Res 14(23):7624–7634. https://doi.org/10.1158/1078-0432.CCR-08-1547
21. Hong JY, An JY, Lee J et al (2020) Claudin 18.2 expression in various tumor types and its role as a potential target in advanced gastric cancer. Transl Cancer Res 9(5):3367–3374. https://doi.org/10.21037/tcr-19-1876
22. Kubota Y, Kawazoe A, Mishima S et al (2023) Comprehensive clinical and molecular characterization of claudin 18.2 expression in advanced gastric or gastroesophageal junction cancer. ESMO Open 8(1):100762. https://doi.org/10.1016/j.esmoop.2022.100762
23. Dottermusch M, Kruger S, Behrens HM et al (2019) Expression of the potential therapeutic target claudin-18.2 is frequently decreased in gastric cancer: results from a large Caucasian cohort study. Virchows Arch 475(5):563–571. https://doi.org/10.1007/s00428-019-02624-7
24. Wang C, Wu N, Pei B et al (2023) Claudin and pancreatic cancer. *Front*. Oncol 13:1136227. https://doi.org/10.3389/fonc.2023.1136227
25. Moentenich V, Gebauer F, Comut E et al (2020) Claudin 18.2 expression in esophageal adenocarcinoma and its potential impact on future treatment strategies. Oncol Lett 19(6):3665–3670. https://doi.org/10.3892/ol.2020.11520
26. Sahin U, Schuler M, Richly H et al (2018) A phase I dose-escalation study of IMAB362 (Zolbetuximab) in patients with advanced gastric and gastro-oesophageal junction cancer. Eur J Cancer 100:17–26. https://doi.org/10.1016/j.ejca.2018.05.007
27. Shah MA, Ajani JA, Al-Batran S-E, et al (2020) Phase III study of first-line zolbetuximab + CAPOX versus placebo + CAPOX in Claudin 18.2+/HER2−advanced or metastatic gastric or gastroesophageal junction adenocarcinoma: GLOW. 38(15_suppl):TPS4648-TPS48. doi: https://doi.org/10.1200/JCO.2020.38.15_suppl.TPS4648
28. Shitara K, Lordick F, Bang Y-J, et al. (2023) Zolbetuximab + mFOLFOX6 as first-line (1L) treatment for patients (pts) with claudin-182+ (CLDN182+)/HER2−locally advanced (LA) unresectable or metastatic gastric or gastroesophageal junction (mG/GEJ) adenocarcinoma: Primary results from phase 3 SPOTLIGHT study. 41(4_suppl):LBA292–LBA92. https://doi.org/10.1200/JCO.2023.41.4_suppl.LBA292
29. Shah MA, Shitara K, Ajani JA et al (2023) Zolbetuximab plus CAPOX in CLDN18.2-positive gastric or gastroesophageal junction adenocarcinoma: the randomized, phase 3 GLOW trial. Nat Med. https://doi.org/10.1038/s41591-023-02465-7
30. Gong J, Li N, Guo W et al (2022) A phase I study of TST001, a high affinity humanized anti-CLDN18.2 monoclonal antibody, in combination with capecitabine and oxaliplatin (CAPOX) as a first-line treatment of advanced G/GEJ cancer. J Clin Oncol 40(16_suppl):4062. https://doi.org/10.1200/JCO.2022.40.16_suppl.4062
31. Gao J, Wang Z, Jiang W et al (2023) CLDN18.2 and 4–1BB bispecific antibody givastomig exerts antitumor activity through CLDN18.2-expressing tumor-directed T-cell activation. J Immunother Cancer. https://doi.org/10.1136/jitc-2023-006704
32. Qi C, Gong J, Li J et al (2022) Claudin18.2-specific CAR T cells in gastrointestinal cancers: phase 1 trial interim results. Nat Med 28(6):1189–1198. https://doi.org/10.1038/s41591-022-01800-8

33. Tian Z, Liu M, Zhang Y et al (2021) Bispecific T cell engagers: an emerging therapy for management of hematologic malignancies. J Hematol Oncol 14(1):75. https://doi.org/10.1186/s13045-021-01084-4
34. Mester S, Evers M, Meyer S et al (2021) Extended plasma half-life of albumin-binding domain fused human IgA upon pH-dependent albumin engagement of human FcRn in vitro and in vivo. MAbs 13(1):1893888. https://doi.org/10.1080/19420862.2021.1893888
35. Zhong W, Lu Y, Ma Z et al (2022) Development of a humanized VHH based recombinant antibody targeting claudin 18.2 Positive cancers. Front Immunol 13:885424. https://doi.org/10.3389/fimmu.2022.885424
36. Li R, Yang H, Jia D et al (2016) Fusion to an albumin-binding domain with a high affinity for albumin extends the circulatory half-life and enhances the in vivo antitumor effects of human TRAIL. J Control Release 228:96–106. https://doi.org/10.1016/j.jconrel.2016.03.004
37. Xu Y, Fu J, Henderson M et al (2023) CLDN18.2 BiTE engages effector and regulatory T cells for antitumor immune response in preclinical models of pancreatic cancer. Gastroenterology 165(5):1219–1232. https://doi.org/10.1053/j.gastro.2023.06.037
38. Cao W, Xing H, Li Y et al (2022) Claudin18.2 is a novel molecular biomarker for tumor-targeted immunotherapy. Biomark Res 10(1):38. https://doi.org/10.1186/s40364-022-00385-1
39. Sitarz R, Skierucha M, Mielko J et al (2018) Gastric cancer: epidemiology, prevention, classification, and treatment. Cancer Manag Res 10:239–248. https://doi.org/10.2147/CMAR.S149619
40. Yadav D, Lowenfels AB (2013) The epidemiology of pancreatitis and pancreatic cancer. Gastroenterology 144(6):1252–1261. https://doi.org/10.1053/j.gastro.2013.01.068
41. Yura M, Takahashi T, Fukuda K et al (2018) A highly advanced gastric cancer maintaining a clinical complete response after chemoradiotherapy comprising s-1 and cisplatin. Case Rep Gastroenterol 12(3):578–585. https://doi.org/10.1159/000492206
42. Von Hoff DD, Ervin T, Arena FP et al (2013) Increased survival in pancreatic cancer with nab-paclitaxel plus gemcitabine. N Engl J Med 369(18):1691–1703. https://doi.org/10.1056/NEJMoa1304369
43. Klein-Brill A, Amar-Farkash S, Lawrence G et al (2022) Comparison of FOLFIRINOX vs gemcitabine plus nab-paclitaxel as first-line chemotherapy for metastatic pancreatic ductal adenocarcinoma. JAMA Netw Open 5(6):e2216199. https://doi.org/10.1001/jamanetworkopen.2022.16199
44. Shitara K, Lordick F, Bang YJ et al (2023) Zolbetuximab plus mFOLFOX6 in patients with CLDN18.2-positive, HER2-negative, untreated, locally advanced unresectable or metastatic gastric or gastro-oesophageal junction adenocarcinoma (SPOTLIGHT): a multicentre, randomised, double-blind, phase 3 trial. Lancet 401(10389):1655–1668. https://doi.org/10.1016/S0140-6736(23)00620-7
45. Chen J, Xu Z, Hu C et al (2023) Targeting CLDN18.2 in cancers of the gastrointestinal tract: New drugs and new indications. Front Oncol 13:1132319. https://doi.org/10.3389/fonc.2023.1132319
46. Morris EC, Neelapu SS, Giavridis T et al (2022) Cytokine release syndrome and associated neurotoxicity in cancer immunotherapy. Nat Rev Immunol 22(2):85–96. https://doi.org/10.1038/s41577-021-00547-6
47. Iwata Y, Sasaki M, Harada A et al (2019) Daily ascending dosing in cynomolgus monkeys to mitigate cytokine release syndrome induced by ERY22, surrogate for T-cell redirecting bispecific antibody ERY974 for cancer immunotherapy. Toxicol Appl Pharmacol 379:114657. https://doi.org/10.1016/j.taap.2019.114657
48. Zhang X, Fu Z, Yan C (2022) Cytokine release syndrome induced by pembrolizumab: a case report. Medicine (Baltimore) 101(49):e31998. https://doi.org/10.1097/MD.0000000000031998